

# Holographic lens — study of imaging quality\*

M. ZAJĄC, J. NOWAK, A. GADOMSKI

Institute of Physics, Technical University of Wrocław, Wybrzeże Wyspiańskiego 27, 50-370 Wrocław, Poland.

Aberration properties of holographic lenses are analysed. The conditions for aplanatic correction are derived and other possibilities of imaging quality improving are checked: the recording of the holo-lens on a curved surface, which allows to compensate coma, and the shifting of the input pupil to compensate astigmatism. The obtained results are illustrated with numerically calculated two-dimensional characteristics of the image, such as the light intensity distribution in the aberration spot, incoherent Transfer Function or coherent image of the Ronchi ruling.

## 1. Introduction

Nowadays in modern optics unconventional imaging elements are more and more widely used in practice. The holographic lens can serve as a good example.

The holographic lens (holo-lens) is, in fact, an on-line hologram, or a photographically recorded system of concentric fringes resulting from interference of two spherical light waves diverging from point sources  $P_1$  and  $P_R$  located on the axis perpendicular to the holo-lens plane. Such a holo-lens makes it possible to transform a spherical light wave diverging from a point  $P_C$  into two spherical waves with centres in points  $P'_3$  i  $P''_3$ . These points can be therefore treated as (primary and secondary) images of a point source  $P_C$ .

As a holo-lens is a kind of hologram so aberration-free imaging is possible in principle. However, such a situation can occur only for a certain specific configuration of points  $P_1$ ,  $P_R$  and  $P_C$ ; in particular, the point object  $P_C$  must lie on the holo-lens axis. In general, if object is extended or located off the axis, its image will be deformed.

The question of the imaging quality obtained by holographic lens have been investigated by many workers; a series of our papers [1]–[4] has been devoted to this subject as well. In this paper further results are given and an attempt of systematization is been presented as a kind of summary.

First let us recall some basic ideas and introduce notation.

Let the holo-lens be recorded with monochromatic light of wavelength  $\lambda_1$  in the

---

\* This work has been sponsored by the Polish Ministry of National Education, Project CPBP 01.06, and was presented at the VIII Polish-Czechoslovakian Optical Conference, Szklarska Poręba (Poland), September 13–16, 1988.

optical system, as presented in Fig. 1a. The letters  $z_1$  and  $z_R$  denote the distances from the point sources  $P_1$  and  $P_R$  (located on axis  $OZ$ ) from the holo-lens plane  $XOY$ .

When imaging takes place in monochromatic light of wavelength  $\lambda_2$  (the notation  $\lambda_2/\lambda_1 = \mu$  will be used from now on) the point object  $P_c$  is located off the axis, in the plane  $XOZ$  being the meridional one (Fig. 1b). Its rectangular coordinates are

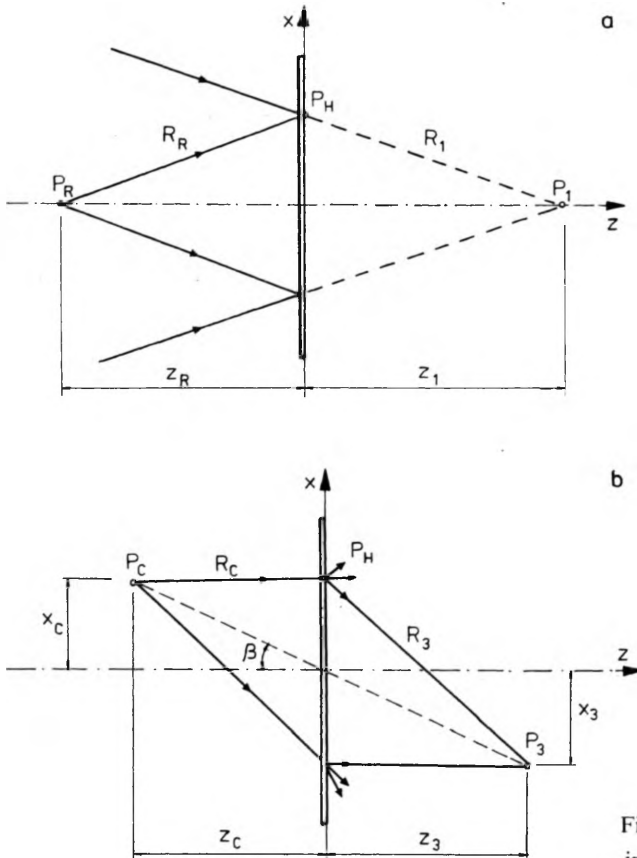


Fig. 1. Geometry of the holo-lens recording (a) and imaging (b)

therefore  $(x_c, 0, z_c)$ . Only one image (primary)  $P_3$  of coordinates  $(x_3, 0, z_3)$  is of our interest. An arbitrary point in the entrance pupil of the holo-lens is denoted by  $P_H(x, y, 0)$ . The letter  $R$  with indices 1, R, C or 3 denote the respective distances from the points  $P_1, P_R, P_C$  or  $P_3$ , to the point  $P_H$ . The ratio  $x_c/z_c = \beta$  describes the field angle in the object space. It is assumed throughout this paper that the scale of the holo-lens used for imaging remains unchanged with respect to its scale during the lens recording process (i.e., the scaling factor  $m = 1$ ).

To describe the optical parameters of the holographic lens it is convenient to use the Meier's expansion [5], [6] widely employed in holography. Such a simplification is admissible if the aperture and field angles are small.

Focal length of the holo-lens is then

$$f = \pm \frac{1}{\mu} \left( \frac{1}{z_1} - \frac{1}{z_R} \right)^{-1} \quad (1)$$

where the upper and lower signs correspond to the primary and secondary images, respectively (as in the sequel).

Coordinates of the Gaussian image can be calculated from the following expressions:

$$\frac{1}{z_3} = \frac{1}{z_C} + \frac{1}{f}, \quad (2)$$

$$\frac{x_3}{z_3} = \frac{x_C}{z_C}.$$

The wave aberration in the 3rd-order approximation can be expressed as

$$W = -\frac{1}{8}(x^2 + y^2)^2 S + \frac{1}{2}(x^2 + y^2) x C_x - \frac{1}{2}(x^2 + y^2) x^2 A_x - \frac{1}{2}(x^2 + y^2) A_x \quad (3)$$

where  $x, y$  are the coordinates of the point  $P_H$  in the entrance pupil, and  $S, C_x, A_x$  are the only non-zero aberration coefficients describing spherical aberration, coma and astigmatism, respectively:

$$S = \frac{1}{z_C^3} \pm \mu \left( \frac{1}{z_1^3} - \frac{i}{z_R^3} \right) - \frac{1}{z_3^3},$$

$$C_x = \frac{x_C}{z_C^3} - \frac{x_3}{z_3^3} = -\frac{x_C}{z_C} \frac{1}{f} \left( \frac{1}{f} + \frac{2}{z_C} \right), \quad (4)$$

$$A_x = \frac{x_C^2}{z_C^3} - \frac{x_3^2}{z_3^3} = -\frac{x_C^2}{z_C^2} \frac{1}{f}.$$

Distortion does not occur and field curvature is expressed by  $A_x$ .

The estimation of the imaging quality by analysis of the 3rd-order aberration coefficients is often completed by using the ray-tracing through the holo-lens or by the spot diagram calculation. To this end the algorithm and the computer programme developed by us for the holographic imaging can be adapted [7].

The mentioned above "geometrical" methods of imaging quality estimation are generally not sufficient and therefore it may be necessary to enrich them by calculation of the light intensity distribution in the aberration spot or in the image of some test object.

The light intensity distribution in the image of a point can be calculated numerically with the aid of another algorithm and computer programme developed by us and presented in [8]. For incoherent illumination it is useful also to compute the Optical Transform Function. Interesting information about coherent imaging of the extended objects can be deduced from the light intensity distribution in the image

of the Ronchi ruling calculated numerically from the complex aberration spot, what can be done if local isoplanatism is assumed [2], [6].

Such a numerical modelling of the image-forming process by the holographic lens may be applied to imaging quality estimation and will be used in the following sections of the paper. In the contrary to our previous papers all the calculations are conducted two-dimensionally, therefore the exploited numerical model simulates the real imaging process with much better accuracy.

The problem of aberration correction of the holo-lens will be investigated and those methods will be used for verification and illustration of the obtained results.

## 2. Aplanatic correction

It is well known that in order to assure a good imaging, for not too great field angles, an aplanatic correction is suitable. To obtain such a correction it is necessary to fulfil the sine condition and to compensate spherical aberration simultaneously [9].

Using the notation already introduced it is possible to formulate the sine condition as follows (cp. Eq. (2)):

$$\frac{\sin u_3}{\sin u_C} = \frac{x_3}{x_C} = \frac{z_3}{z_C}. \quad (5)$$

The relation between angles  $u_3$  and  $u_C$  is simple (cp. [10]) and in the meridional plane it can be written down as

$$\sin u_3 = \sin u_C \pm \lambda_2/D_x \quad (6)$$

where  $D_x^{-1}$  is the local spatial frequency of fringes on the holo-lens, given by

$$D_x = \frac{x(R_R - R_1)}{\lambda_1(R_1 R_R)}. \quad (7)$$

By combining the above formulae it is easy to obtain

$$\frac{\sin u_3}{\sin u_C} = 1 \pm \mu R_C \left( \frac{1}{R_1} - \frac{1}{R_R} \right). \quad (8)$$

Let  $\Delta$  be the deviation from the sine condition. Then after straightforward calculations one can obtain

$$\Delta = \frac{z_C}{f} \mp \mu R_C \left( \frac{1}{R_1} - \frac{1}{R_R} \right) \quad (9)$$

where  $f$  is the holo-lens focal length.

It can be easily shown that if the spherical aberration is compensated for  $\mu = 1$  (for that  $z_C = \pm z_R$  is sufficient, see [10]), and additionally  $z_R = -z_1$ , then the sine condition is also fulfilled ( $\Delta = 0$ ) and the holo-lens is aplanatic.

However, the possibility of an aplanatic correction for  $\mu \neq 1$  is also of interest. Because of spectral properties of the light-sensitive materials used for the holo-lens

recording different light wavelengths are sometimes used during lens recording and its imaging.

To find adequate conditions for aberration correction in such a situation it is more convenient to require a simultaneous vanishing of spherical aberration and coma rather than to start with the analysis of sine condition.

Taking into account Eqs. (1)–(3) it is possible to rewrite the respective aberration coefficients in the form:

$$S = \pm \mu(1 - \mu^2) \left( \frac{1}{z_1^3} - \frac{1}{z_R^3} \right) - \frac{3\mu^2}{z_C} \left( \frac{1}{z_1} - \frac{1}{z_C} \right)^2 \mp 3\mu \left( \frac{1}{z_C^2} - \frac{\mu^2}{z_1 z_R} \right) \left( \frac{1}{z_1} - \frac{1}{z_R} \right), \tag{10}$$

$$C_x = -\frac{x_C}{z_C f} \left( \frac{1}{f} + \frac{2}{z_C} \right). \tag{11}$$

The postulate  $C_x = 0$  leads to the condition

$$z_C = -2f. \tag{12}$$

The spherical aberration vanishes when

$$\frac{z_1}{z_C} = \mp \frac{1}{2} \mu \left( 1 - \frac{z_1}{z_R} \right) - \frac{1}{6\sqrt{9\mu^2 \left( 1 - \frac{z_1}{z_R} \right)^2 \pm \frac{12}{1 - z_1/z_R} \left[ \mp \mu^2 \left( 1 - \frac{z_1}{z_R} \right)^3 \mp \left( \frac{z_1}{z_R} \right)^3 \pm 1 \right]}}$$

or

$$\begin{aligned} \frac{z_1}{z_C} = & \mp \frac{1}{2} \mu \left( 1 - \frac{z_1}{z_R} \right) \\ & + \frac{1}{6\sqrt{9\mu^2 \left( 1 - \frac{z_1}{z_R} \right)^2 \pm \frac{12}{1 - z_1/z_R} \left[ \mp \mu^2 \left( 1 - \frac{z_1}{z_R} \right)^3 \mp \left( \frac{z_1}{z_R} \right)^3 \pm 1 \right]}}. \end{aligned} \tag{13}$$

By combining Equations (12) and (13), one can obtain the relation between the ratio  $z_1/z_R$  and the coefficient  $\mu$  ensuring the aplanatic correction

$$\mu = 2 \sqrt{\frac{1 - (z_1/z_R)^3}{(1 - z_1/z_R)^3}}. \tag{14}$$

This formula is illustrated by a graph shown in Fig. 2. It is clearly seen that, apart from the well known condition for  $\mu = 1$ , there exist a number of other possibilities for aplanatic correction. To this end a proper value of the  $z_1/z_R$  ratio during the holo-lens recording step should be properly chosen according to the expected value of  $\mu$ .

In particular, when  $\mu = 2$  is chosen (which is a reasonable value even if only visible part of the light spectrum is taken into account) an aplanatic telescopic lens may be obtained. By “telescopic lens” we mean that the plane wave falling on this lens is focused in the focal plane.

The other geometries of the holo-lens recording are also possible according to the value of  $\mu \neq 1$ .

To illustrate the above possibilities of an aplanatic correction let us analyse the

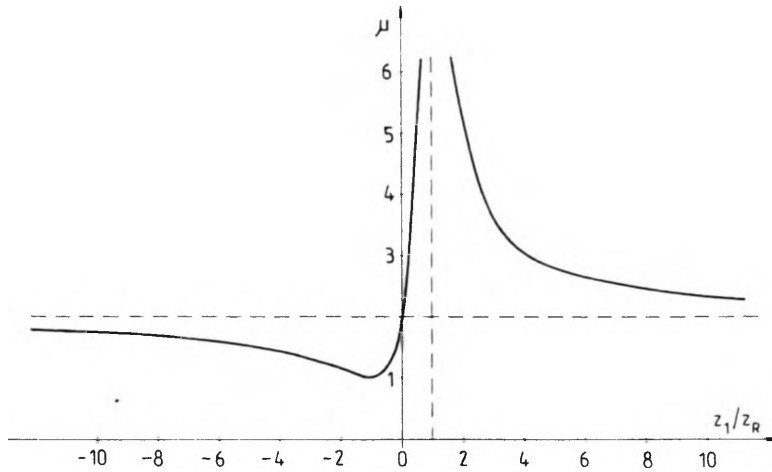


Fig. 2. Dependence of  $\mu$  vs  $z_1/z_R$  assuring the aplanatic correction

imaging by several exemplary aplanatic lenses. Four geometries of the holo-lens recording and imaging assuring the aplanatic correction are chosen. The values of  $\mu$ ,  $z_1$  and  $z_R$  are given in Tab. 1 (all distances in tables and figures are given in millimeters). All lenses have the same focal length  $f = 100$  mm. The magnitude of their pupils assures a constant aperture angle in the image space  $u_3 = 0.1$ .

Table 1. Geometry parameters of the investigated holo-lenses

No.	$\mu$	$z_1$	$z_R$	$z_C$	$z_3$	$\varrho$	$t$	$D$
I-1	1	200	-200	-200	199.91	$\infty$	0	20
I-2	2	200	$\infty$	$\infty$	99.91	$\infty$	0	10
I-3a	1.5275	916.12	-183.28	-200	199.91	$\infty$	0	20
I-3b	1.5275	183.28	-916.12	-200	199.91	$\infty$	0	20
II	1	150	-300	-300	149.91	$\infty$	0	15
III-1	1	100	$\infty$	$\infty$	99.91	$\infty$	0	10
III-2	1	100	$\infty$	$\infty$	99.91	$\infty$	-50	10
III-3	1	100	$\infty$	$\infty$	99.91	100	0	10

As the holographic lens is burdened with field curvature, it is necessary to choose properly the plane of image analysis. In general, it is not a Gaussian image plane. In the present paper the image is investigated in an "optimum" plane, perpendicular to the optical axis, but shifted with respect to the Gaussian plane, so the Strehl ratio for the point on axis is not less than 0.8, i.e., the Marechal criterion is fulfilled. The shift amounts to about 0.05% of the Gaussian image distance. The chosen value of  $z_3$  is also given in the table.

The holo-lens No. I-1 is the typical aplanatic one ( $\mu = 1$ ), the lens No. I-2 is the telescopic one ( $\mu = 2$ ), and the lenses No. I-3a and No. I-3b represent the intermediate cases.

In terms of the 3rd-order aberrations all those lenses have the same aberration characteristics. The coefficients of spherical aberration and coma are equal to zero, the astigmatism differs from zero being the same for equal field angles.

The numerically calculated light intensity distribution in the image of a point (i.e., in the aberration spot), the wave aberration, the incoherent Optical Transfer Function (its modulus – MTF – being drawn with solid line and the phase – PTF – with dashed one) and the light intensity distribution in the coherent image of Ronchi ruling of the spatial frequency  $\nu = 20$  l/mm for three field angles ( $\beta = 0, 0.01$  and  $0.02$ ) are shown in Fig. 3. For simplicity only the aberration spots are presented in the 3-D graphs; the other curves are presented as the respective meridional cross-sections, which is quite sufficient for the evaluation of the influence of aberration on the image quality.

The results obtained for all the analysed aplanatic lenses are almost identical (for equal field angles) the differences being smaller than the computation accuracy. It is obvious, since the aberration correction of each of the exemplary lenses is the same. Therefore there is no need to multiply the amount of the presented results; but it is quite sufficient to show here the imaging characteristics only once for a “typical aplanatic lens”.

Some numerical parameters characterizing the aberration spot are collected in Tab. 2.

Table 2. Selected parameters of aberration spots for the investigated holo-lenses

No.	$x_C/z_C$	$I_{max}$	$x_3 - \bar{x}$ [ $\times 10^{-3}$ ]	$M_{2x}$ [ $\times 10^{-5}$ ]	$M_{2y}$ [ $\times 10^{-5}$ ]	$M_{3x}$ [ $\times 10^{-7}$ ]	$d_{0.8}$ [ $\times 10^{-3}$ ]	$A_x$ [ $\times 10^{-6}$ ]	$C_x$ [ $\times 10^{-6}$ ]	$\langle W \rangle$ [ $\times 10^{-3}$ ]
I	0	.80	0	1.83	1.83	0	6	0	0	1.06
	0.02	.73	0	1.63	1.75	0	6	-4	0	1.25
	0.03	.20	0	1.82	15.89	0	16	-9	0	3.80
II	0	.80	0	1.83	2.25	0	8	0	0	1.06
	0.02	.86	-3.4	1.70	2.80	-1.62	8	-4	-0.7	1.03
	0.03	.47	-5.1	1.89	6.62	-4.57	10	-9	-1	2.21
III-1	0	.80	0	1.83	1.83	-0	6	0	0	1.06
	0.03	.79	-5.6	1.88	2.72	0.03	8	-9	-3	1.20
	0.04	.56	-9.0	2.10	4.84	1.61	10	-16	-4	1.92
III-2	0	.80	0	1.83	1.83	0	6	0	0	1.06
	0.03	.70	-6.1	2.24	3.26	-1.65	8	0	-3	1.55
	0.04	.60	-8.5	2.54	3.97	-2.29	8	0	-4	1.99
III-3	0	.80	0	1.82	1.82	0	6	0	0	1.06
	0.03	.75	0	2.43	2.13	0.42	6	-9	0	1.19
	0.04	.66	0	3.07	2.00	0.75	6	-16	0	1.42
Aberration free		1.00	0	1.33	1.33	0	4	0	0	0

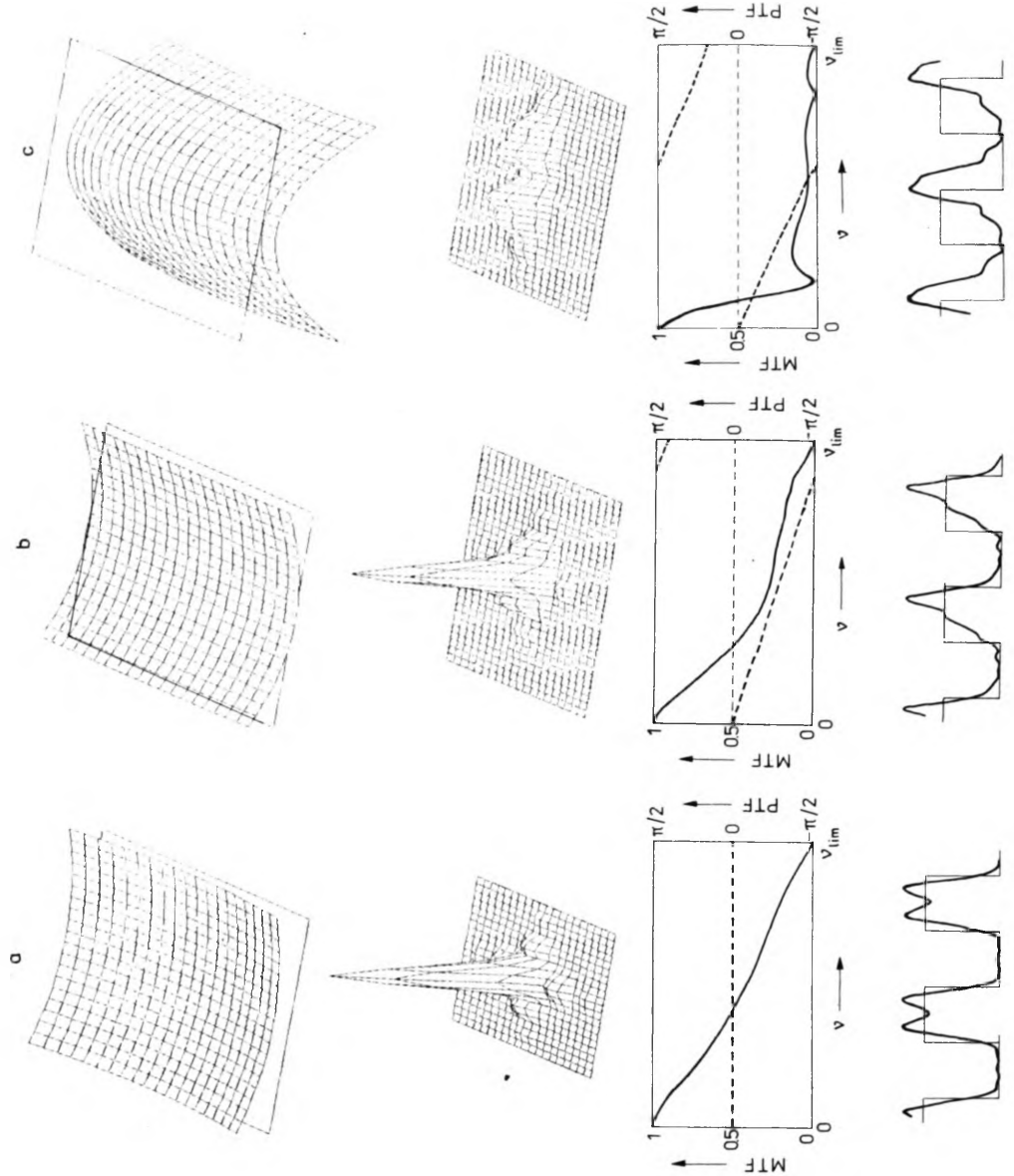


Fig. 3. Wave aberrations, aberration spots, incoherent Modulation Transfer Function and coherent images of Ronchi ruling of spatial frequency  $\nu = 20$  l/mm for the aplanatic holo-lens and different field angles (a -  $x_c/z_c = 0$ , b -  $x_c/z_c = 0.2$ , c -  $x_c/z_c = 0.3$ )

$I_{\max}$  — normalised light intensity in the centre of the aberration spot (Strehl ratio),

$x_3 - \bar{x}$  — distance from the Gaussian image to the aberration spot centre of gravity ( $y_3 - \bar{y} \equiv 0$ ),

$M_{2x} = \frac{\int I(x, y)(x - \bar{x})^2 dx dy}{\int I(x, y) dx dy}$ ,  $M_{2y} = \frac{\int I(x, y)(y - \bar{y})^2 dx dy}{\int I(x, y) dx dy}$ , — second-order moments of the light intensity distribution in aberration spot describing its “flatness”:

$M_{3x} = \frac{\int I(x, y)(x - \bar{x})^3 dx dy}{\int I(x, y) dx dy}$  — third-order moment of the light intensity distribution in the aberration spot being a measure of its asymmetry ( $M_{3y} \equiv 0$ );

$d_{0.8}$  — diameter of a circle containing 80% of the light energy in the aberration spot (strictly speaking it is one side of the respective square, because the holo-lens aperture is assumed to be square-shaped).

The only non-zero aberration coefficient  $A_x$  as well as the mean square value of wave aberration  $\langle W \rangle$  (calculated with respect to the reference sphere centered in the aberration spot center of gravity and measured in fractions of  $\lambda$ ) are also given in this table.

The presented results show that the aplanatic correction has been really obtained. The aberration spots are symmetrical and the phase of Optical Transfer Function (PTF) is linear — there is no coma seen. However, the imaging quality may be treated as being satisfactory only for the objects located not too far from the holo-lens axis. Even for such relatively small field angles, such as  $u_C = 0.02$ , the imaging quality deteriorates significantly ( $I_{\max} \approx 0.2$ ).

### 3. Non-aplanatic holographic lenses

The final conclusion of the previous Section suggests the necessity of searching another possibility of aberration correction, enabling us to obtain a better imaging quality. For this purpose another holo-lens geometry may be employed; the aplanatic correction existing no longer.

For a more detailed investigation of such a possibility of aberration correction, two other types of holographic lenses have been analysed. No. II denotes the holo-lens in which  $z_R = -2z_1$  is chosen, No. III-1 denotes a telescopic lens which was recorded with one light source in infinity. This lens can be used for focusing the parallel beams of light. Spherical aberration of both lenses may be compensated if  $z_C = \pm z_R$ . In both the cases  $\mu = 1$ , the distances  $z_1$ ,  $z_R$  and the size of the entrance pupil are chosen in such a way, that the focal length of both lenses  $f = 100$  mm and the aperture angle in image space  $u_3 = 0.1$ . Therefore the resulting images might be directly compared with those given by the previously analysed aplanatic lens which can serve for comparative purposes.

All the geometric parameters of the analysed lenses are collected also in Tab. 1.

The same imaging characteristics as those for the aplanatic holo-lens but, for the holo-lenses No. II and No. III-1 and different field angles are presented in Figs. 4 and 5 — all in the image plane best chosen for each lens.

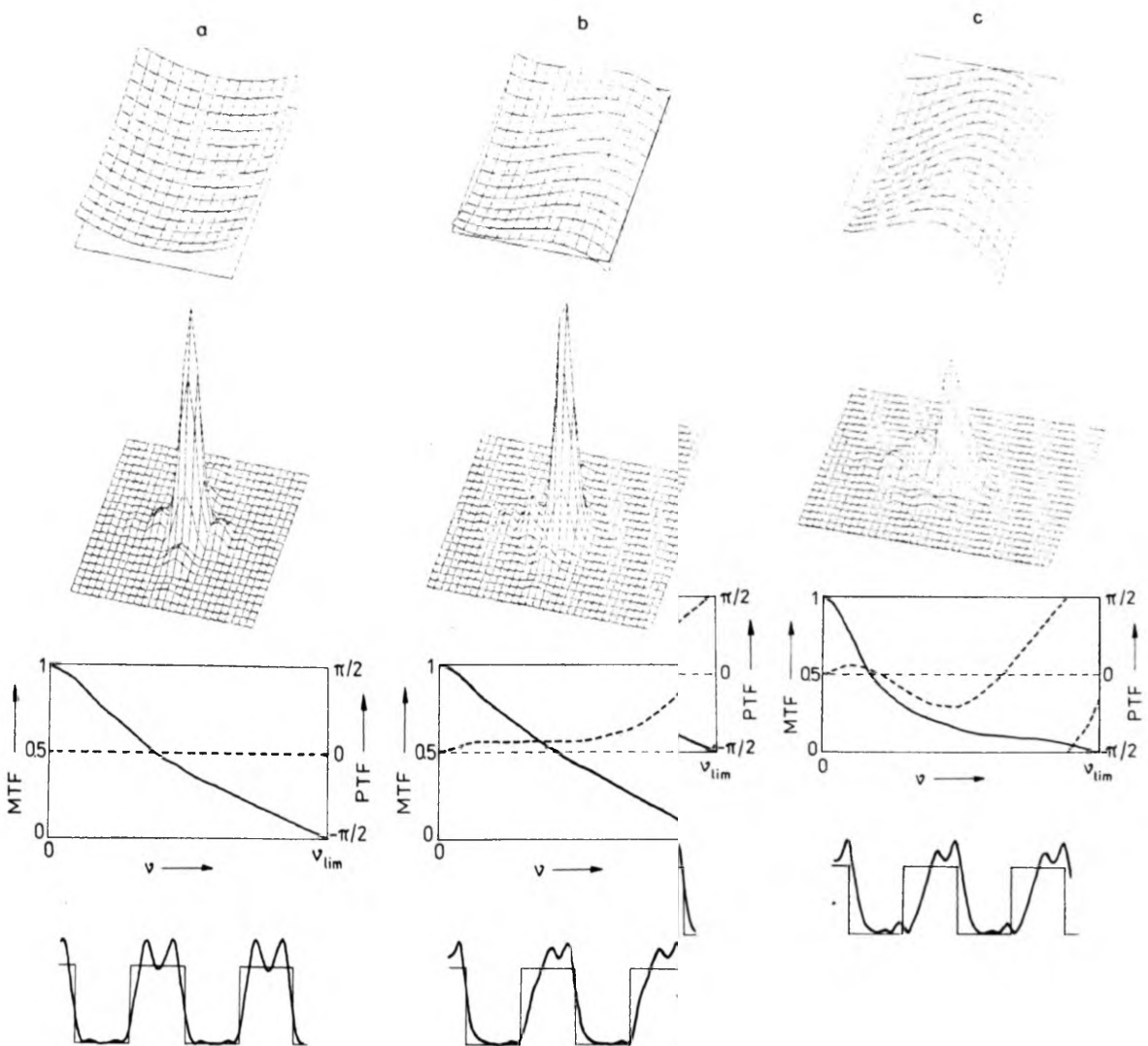


Fig. 4. The same as in Fig. 3, but for the holo-lens No. II (a —  $x_c/z_c = 0$ , b —  $x_c/z_c = 0.2$ , c —  $x_c/z_c$

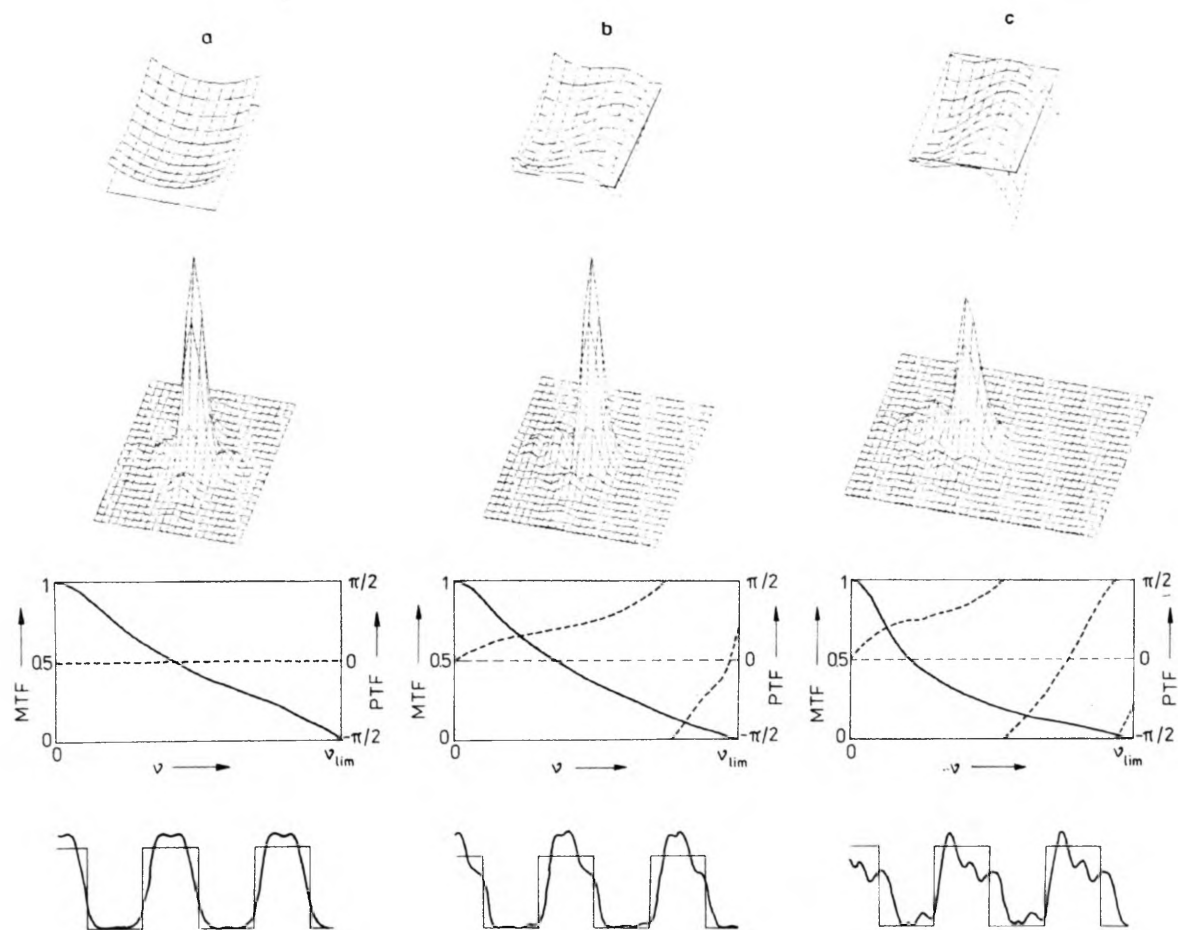


Fig. 5. The same as in Fig. 3, but for the holo-lens No. III-1 (a -  $x_c/z_c = 0$ , b -  $x_c/z_c = 0.3$ , c -  $x_c/z_c = 0.3$ )

Numerical characteristics of the aberration spots, shown in consecutive columns of Tab. 2, are the same as these in the previous case. From the analysis of these data it follows that the aplanatic lens has a good imaging quality only for field angles not exceeding the value of 0.02. In the holo-lenses No. II and No. III the astigmatism coefficient is smaller, but there appears uncorrected coma. It can be seen in some asymmetries in the wave aberration as well as in the aberration spot deformation. The phase of the Optical Transfer Function is linear. The imaging, however, seems to be a little better than the one for the aplanatic lens. This is visible especially for the field angle equal to 0.03. For the lens No. III-1 it is even possible to consider the field angle as large as 0.04.

The possibilities of aberration correction are not exhausted. There exists also a possibility of the holo-lens recording on a curved surface (spherical for instance [3], [4], [11]–[18] as well as of shifting its entrance (or exit) pupil out of its plane [13], [19]–[22], cp. Fig. 6.

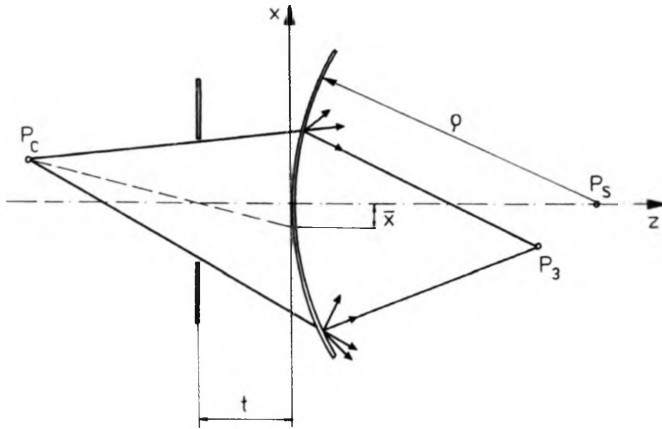


Fig. 6. Geometry of imaging using the "spherical" holo-lens with a shifted entrance pupil

In this way, there appear two additional quantities: the curvature radius of the holo-lens surface  $\rho$  and the shift  $t$  of the entrance pupil. The above values influence the aberrations and may be used as additional correction parameters.

Using the Meier's expansion it is possible to express the 3rd-order aberration coefficients of the holo-lens recorded on the curved surface with curvature radius  $\rho$ , as follows:

$$\begin{aligned}
 S_{\rho} &= S_0 + \frac{2}{\rho} \left[ \frac{1}{z_C^2} + \mu \left( \frac{1}{z_1^2} - \frac{1}{z_R^2} \right) - \frac{1}{z_3^2} \right], \\
 C_{x,\rho} &= C_{x,0} + \frac{1}{\rho} \left( \frac{x_C}{z_C^2} - \frac{x_3}{z_3^2} \right), \\
 A_{x,\rho} &= A_{x,0}
 \end{aligned} \tag{15}$$

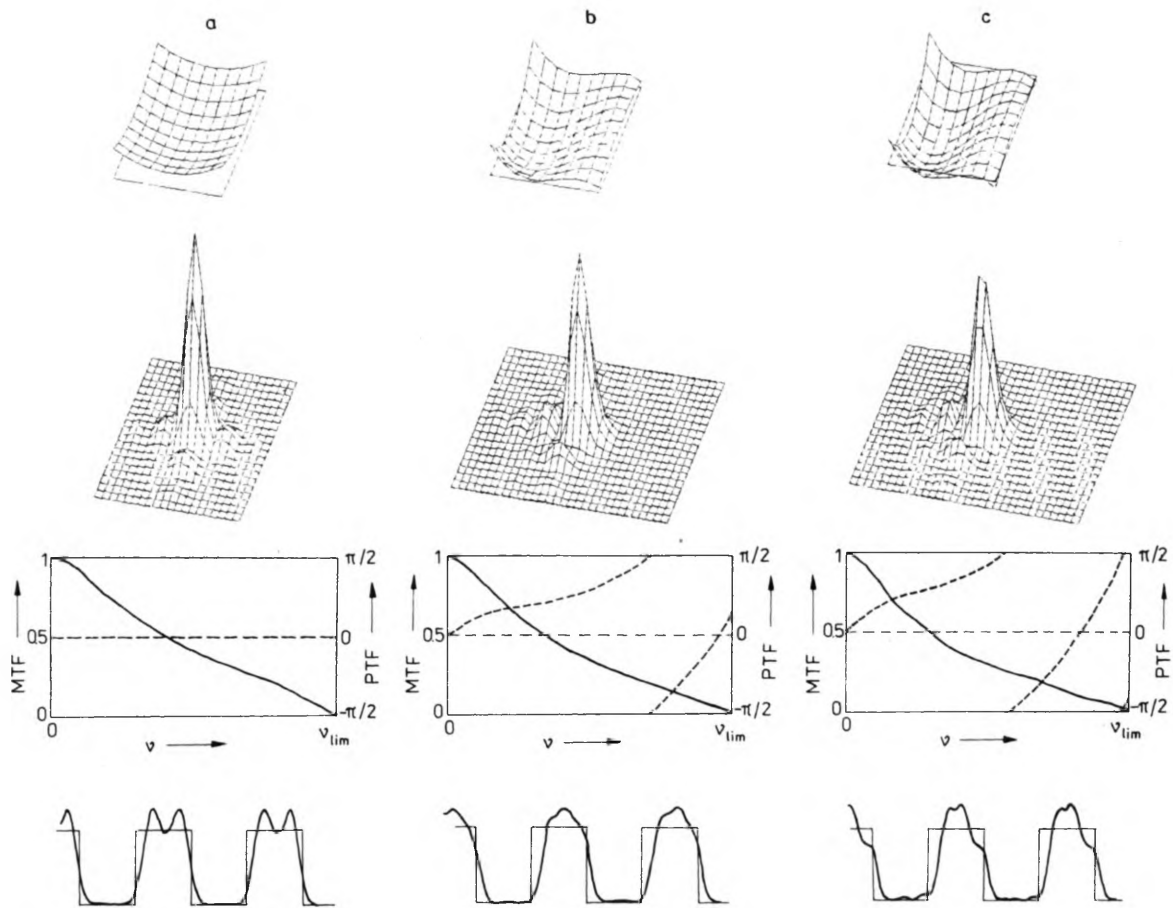


Fig. 7. The same as in Fig. 3, but for the holo-lens No. III-2 (a -  $x_c/z_c = 0$ , b -  $x_c/z_c = 0.3$ , c -  $x_c/z_c = 0.4$ )

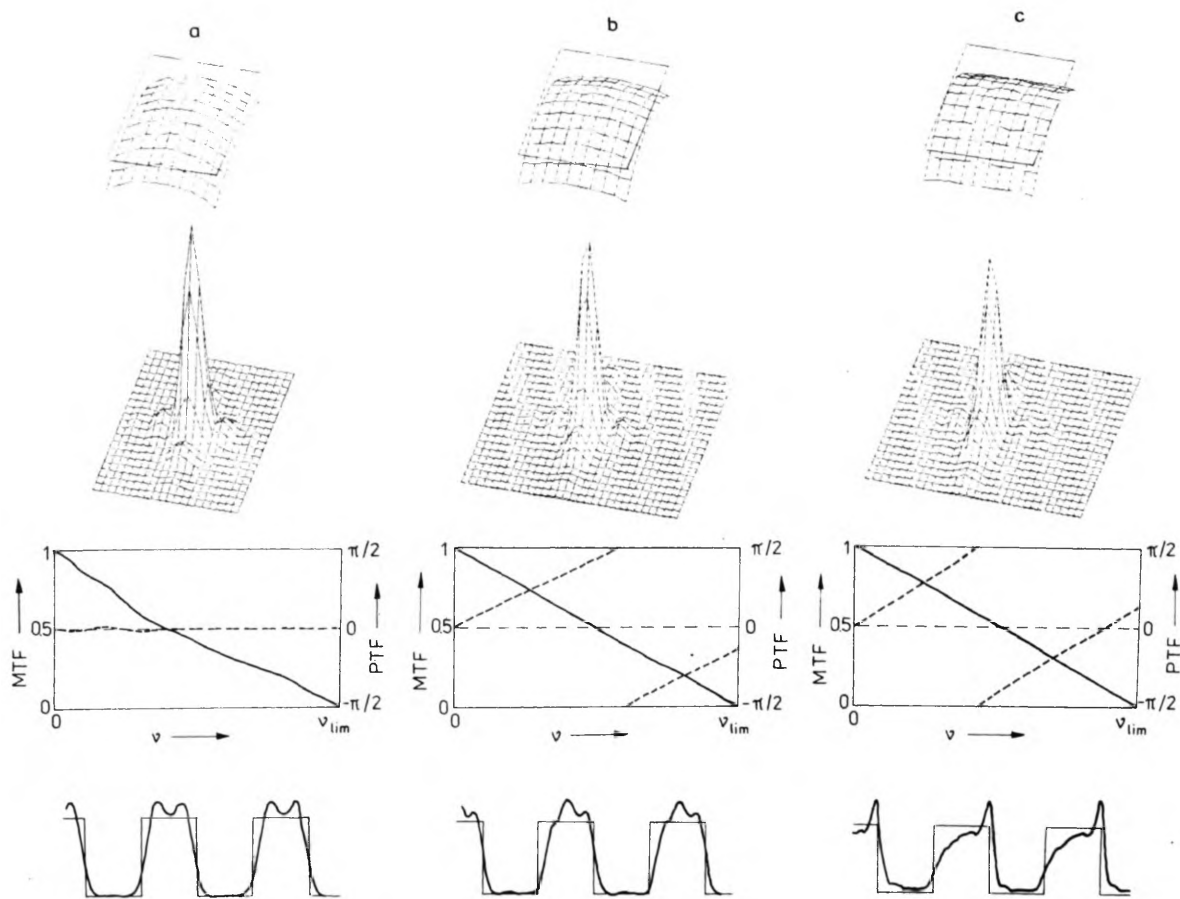


Fig. 8. The same as in Fig. 3, but for the holo-lens No. III-3 (a -  $x_C/z_C = 0$ , b -  $x_C/z_C = 0.3$ , c -  $x_C/z_C = 0.4$ )

where  $S_0$ ,  $C_{x,0}$ ,  $A_{x,0}$  denote the respective coefficients for the flat lens (cp. Eq. (4)).

A shift of the entrance pupil by  $t$  induces the following change in the aberration coefficients:

$$\begin{aligned} S_t &= S_0, \\ C_{x,t} &= C_{x,0} + \bar{x} S_0, \\ A_{x,t} &= A_{x,0} - 2\bar{x} C_{x,0} + \bar{x}^2 S_0 \end{aligned} \quad (16)$$

where

$$\bar{x} = x_c t / (t - z_c) \quad (17)$$

is the apparent displacement of the active area centre of the holo-lens introduced by the pupil shift.

It is easy to notice that in all the investigated cases the spherical aberration is equal to zero for both holo-lenses: the flat one as well for the lens of the curved surface independently of the entrance pupil location. Therefore by recording the holo-lens on the suitably chosen curved surface it is possible to compensate coma fully with unchanged astigmatism. On the other hand, by shifting the input pupil the astigmatism may be compensated without any change in coma.

To illustrate those possibilities of aberrations correction, let us analyse the imaging quality of two modifications of the lens No. III-1 which is undoubtedly the best one. The lens No. III-2 recorded on the flat surface has the pupil shifted sufficiently to correct astigmatism. The lens No. III-3 is recorded on the spherical surface the radius of which assures coma correction. The geometric parameters of those lenses are presented also in Tab. 1.

The calculated image characteristics are illustrated in Fig. 7 (the holo-lens with shifted pupil) and in Fig. 8 (the spherical holo-lens). In Tab. 2 the parameters characterizing the aberration spots and wave aberration are given.

From the presented graphs and tables it follows that a certain improvement of the imaging quality can be obtained. For instance, for the lens No. III-3 in the full range of the analysed field angles the Strehl ratio falls down only slightly below the value 0.8 fulfilling the Marechal criterion and the aberration spot "diameter" (as measured by  $d_{0.8}$ ) exceeds the respective diffraction limited spot diameter only by a factor of two.

#### 4. Summary

The calculations presented here and the illustrating examples indicate that there exists a possibility of designing the holo-lens with corrected aberrations. By recording the holo-lens on a spherical surface and shifting its entrance pupil it is possible to obtain the holo-lenses of quite a good imaging quality for sufficiently large field angles.

On the other hand, the production of the holo-lens on a curved surface may cause some technological troubles. The flat synthetic holo-lens with its adequately

modified fringe distribution might help to overcome this difficulty [23], [24].

Other serious disadvantages follow from small diffraction efficiency of holographic lenses and simultaneous appearance of two images, i.e., primary and secondary ones. It seems that the solution to this problem can be found, as in adoption of the kinoform technology [25].

Both the problems are studied and the results will be reported in the near future.

## References

- [1] NOWAK J., ZAJĄC M., [In] *Proc. Image Science '85 Conf.*, Helsinki 1985, [Eds.] A. Friberg, P.O. Oittinen, add. 56.
- [2] NOWAK J., ZAJĄC M., *Optik* **70** (1985), 143.
- [3] NOWAK J., ZAJĄC M., *Opt. Appl.* **18** (1988), 51.
- [4] ZAJĄC M., NOWAK J., *Optik* (1988), in press.
- [5] MEIER R. W., *J. Opt. Soc. Am.* **55** (1965), 987.
- [6] NOWAK J., Scientific Papers of the Institute of Physics of the Technical University of Wrocław, No. 22, Monographs No. 12, Wrocław 1987 (in Polish).
- [7] NOWAK J., ZAJĄC M., *Optik* **55** (1980), 93.
- [8] NOWAK J., ZAJĄC M., *Opt. Acta* **30** (1983), 1749.
- [9] JÓZWICKI R., *Optyka instrumentalna*, [Ed.] WNT, Warszawa 1970 (in Polish).
- [10] NOWAK J., *Opt. Appl.* **8** (1978), 145.
- [11] MUSTAFIN K. S., *Opt. Spektrosk.* **37** (1974), 1158 (in Russian).
- [12] WELFORD W. T., *J. Phot. Sci.* **23** (1975), 84.
- [13] MUSTAFIN K. S., SATTAROV F. A., *Opt. Spektrosk.* **47** (1979), 1204 (in Russian).
- [14] GAJ M., KŁEK A., *Opt. Appl.* **10** (1980), 341.
- [15] JAGOSZEWSKI E., *Optik* **49** (1985), 85.
- [16] VERBOVEN P. E., LAGASSE P. E., *Appl. Opt.* **25** (1986), 4250.
- [17] WEIGARTNER I., ROSENBRUCH M., *Optik* **73** (1986), 108.
- [18] JAGOSZEWSKI E., PODBIELSKA H., *Optik* **75** (1987), 109.
- [19] SMITH R. W., *Opt. Commun.* **19** (1976), 245.
- [20] BOBROV S. T., et al., *Opt. Spektrosk.* **46** (1979), 153 (in Russian).
- [21] GREJSUKH G. I., et al., *Zh. Tekh. Fiz.* **49** (1979), 1032 (in Russian).
- [22] NOWAK J., ZAJĄC M., *Opt. Appl.* **10** (1981), 285.
- [23] GADOMSKI A., NOWAK J., *Opt. Appl.* **17** (1987), 377.
- [24] GADOMSKI A., ZAJĄC M., NOWAK J., *Opt. Appl.* **19** (1989), 219.
- [25] KORONKEVICH V. P., et al., *Avtometriya*, No. 1 (1985), 4.

*Received November 28, 1988*

## Голографическая линза — исследование качества изображения

В работе проанализированы абберационные свойства голографических линз. Выведены условия апланатической коррекции, а также были проверены другие возможности улучшения качества изображения как: регистрация голо-линзы на закривленной поверхности, что позволяет компенсировать кому и сдвиг входного зрачка, чтобы компенсировать астигматическую абберацию. Полученные результаты проиллюстрированы таковыми цифрово вычисленными двумерными характеристиками изображения как функция рассеяния точки, некогерентная передаточная функция или когерентное изображение штрихового теста.